Materials Research Proceedings **6** (2018) 117-122 doi: http://dx.doi.org/10.21741/9781945291890-19

In Situ Mechanical Behavior of Regenerating Rat Calvaria Bones Under Tensile Load via Synchrotron Diffraction Characterization

Ameni Zaouali[1,*], Baptiste Girault[1], David Gloaguen[1], Fabienne Jordana[2], Marie-José Moya[1], Pierre-Antoine Dubos[1], Valerie Geoffroy[2], Matthias Schwartzkopf[3], Tim Snow[4], Himadri Gupta[5], Olga Shebanova[4], Konrad Schneider[6], Baobao Chang[6]

[1] Institut de Recherche en Génie Civil et Mécanique, GeM (UMR CNRS 6183), Université de Nantes, 58, rue Michel Ange - BP 420, 44606 Saint-Nazaire Cedex, France

[2] Regenerative Medicine and Skeleton, RMeS (UMR_S 1229), Université de Nantes, Faculté d'Odontologie, 1, place Alexis Ricordeau, 44000 Nantes, France

[3] Deutsches Elektronen-Synchrotron (DESY), Notkestr. 85, 22607 Hamburg, Germany

[4] Diamond Light Source Ltd, Diamond House, Harwell Science & Innovation Campus, Didcot, Oxfordshire OX11 0DE, United Kingdom

[5] Institute of Bioengineering, Queen Mary University of London, London, E1 4NS, United Kingdom

[6] Leibniz-Institut für Polymerforschung Dresden e. V, Dresden, 01069, Germany

* ameni.zaouali@etu.univ-nantes.fr

Keywords: Bone Regeneration, Mechanical Properties, Small Angle X-Ray Scattering, Wide Angle X-Ray Scattering, Mineral Crystals

Abstract . The major challenge of Research in bone surgery is to develop strategies to repair large bone defects. Bone grafting technique is the gold standard to fill and heal these kind of defects. This work address the evolution of the mechanical properties as regard to bone regeneration microstructure. Managing such a time dependent (different regeneration step) and spatially resolved (strain field across natural/reconstructed bone interface) process is achieved through a quantitative analysis of the mechanical strain distribution supported by the mineral part of bone architecture (hydroxyapatite - Hap) and crystal microstructural features (size distribution, spatial pattern). SAXS/WAXS (Small- and Wide- Angle X-ray Scattering) experiments will highlight strain distribution respectively in the reconstructed bone's collagen fibrils and minerals, through mechanical state mapping over a surgically created defect under *in situ* tensile testing on samples harvested at different regeneration stages.

Introduction

Today regenerative medicine is moving towards the development of less and less invasive surgical techniques with the objective of reducing morbidity and the duration of hospitalization. Adult stem cells are a very promising avenue in regenerative medicine. Unfortunately, direct injection into the body suffers from major limitations, in particular for osteoarticular and cardiovascular regeneration. It has been shown that after direct injection most of the cells escapes from the injection site or are not displaying the expected physiological functionality. This quest for reduced-invasive surgery has motivated the development of injectable matrices for bone and cartilage tissue engineering. Once implanted, these injectable matrices must be able to settle down, acquire the desired form, and enable oxygen, nutriment and cell diffusion. Indeed,

Materials Research Proceedings **6** (2018) 117-122 doi: http://dx.doi.org/10.21741/9781945291890-19

different types of implants (notably biocomposites) have been developed and adapted in bone tissue engineering. The evaluation of the clinical success of the latter is translated into the quantification of bone formation [1]. However, the microstructural feature evolution of the newly formed bone and its related mechanical behavior after implantation are still poorly understood. This work aims to study the biomechanical properties of healing bone at different stages of regeneration in order to offer tools for implant material optimization in bone engineering and their clinical success evaluation. The major challenge of this work is therefore to correlate time- and space- resolved mechanical behavior of bone to the related microbiological processes and regeneration kinetics. Proposed experiments intend to particularly highlight the distribution of mechanical stresses induced by the reconstruction process and mainly supported by the mineral part of bone architecture (hydroxyapatite - Hap) through mechanical state mapping thanks to X-ray in various regeneration levels until complete reconstruction thanks to samples harvested at different regeneration stages.. This study is achieved through *in situ* tensile testing under SAXS/WAXS synchrotron μ-beam. The size and orientation of bone mineral particles as well as the space distribution of particle agglomerates in rat calvaria defects, were investigated at different healing stages. The resulting two dimensional maps of crystal strain, mean thickness and degree of orientation, revealed the strong correlation between the bone mechanical resistance and the crystal organization.

Materials and methods

Samples. Eighteen white laboratory rats have been used for bone-regeneration tests (11 animals as implantation recipient and 7 rats as donors). Two bilateral defects of 3 mm diameter were created by surgical way in rat calvaria under general anesthesia. Defects were then treated with a mixture of compact bone powder (femoral head) and blood. Rats were then sacrificed by an overdose of CO_2 at 2, 4, 6 and 8 weeks after surgery. The calvaria parallelepiped-shaped specimens ($10 \times 5 \times 0.6$ mm^3) were harvested from the animals and immersed in a 70 % alcohol solution in order to preserve its mechanical attributes. Mechanical investigations were carried out on samples harvested at the different regeneration stages, emblematic of the osseous reconstruction level. Dogbone sample shaped were managed by embedding 2 mm of the end of their longest dimension (10 mm) in a non-invasive, low polymerization temperature, high stiffness resin.

Small and Wide-angle X-ray scattering. X-ray scattering techniques are particularly appropriate for bone ultrastructure analyses [2]. Indeed, they enable to obtain representative and quantitative information on the nanoscale structure as well as on the shape and organization of the organic and inorganic components. At sub-nanometric (crystal) and nanometric (collagen fiber) levels, Wide and Small Angle X-ray Scattering (respectively WAXS and SAXS) have therefore been used to determine microstructural features over different scales. WAXS patterns enable investigations of crystalline structure, crystallographic orientation, mineral particle distribution and averaged crystal size whereas SAXS analysis enable information onto crystal particles aggregates (clusters) set along collagen fibrils such as their size, orientation distribution or mean distances. Using interreticular distances (WAXS) or cluster distances (SAXS) as strain gages, such techniques enable resolving deformation undergone by either Hap or collagen fibrils, respectively. This leads to a two-scale mechanical behavior characterization (Collagen fibers: > 200 nm; crystals: < 10 nm) when a mechanical load is applied. SAXS and WAXS measurements were conducted at the P03 (MiNaXS) beamline at Petra III Light Source (Hamburg, Germany). Ten samples (3 rat specimens × 3 regeneration stages + reference sample) were studied through *in situ* tensile testing in the elastic regime in a step-by step mode (initial mechanical stress state + 4 incremental loads) up to 50 N. For each loading step, SAXS and WAXS measurements were achieved in transmission mode thanks to two Pilatus detectors with scanning steps of 60 μm in a continuous line-scan mode along (longitudinal strain) and perpendicular (transverse strain) to the

Materials Research Proceedings **6** (2018) 117-122 doi: http://dx.doi.org/10.21741/9781945291890-19

tensile axis with 16 × 22 μm^2 spot size and 15 keV beam energy (1.0 Å wavelength). The drawn map ensure an investigation of the strain distribution in both collagen fibrils (SAXS) and Hap nanocrystallites (WAXS) across the interface between natural and regenerated bone over a 2 × 2 mm² area of acquisition (a fourth of the area of interest, symmetrically representative of the entire circular defect).

Data analysis

WAXS data evaluation. Experimental data were processed with DAWN software (Version 2.8, DIAMOND, UK) [3]. In the first place, the 2D WAXS patterns were converted to 1D diffraction patterns (intensity vs. diffraction angle) using azimuthal integration. The position of obtained diffraction peak gives information on the lattice spacing. In fact, Bragg's law gives a relationship between crystallite structure and parameters as determined from x-ray scattering:

$$n\,\lambda = 2d(hkl)\,\sin\theta. \quad (1)$$

Here, d(hkl) is the interreticular distance for a {hkl} plane family, θ is the Bragg's angle, λ is the X-ray wavelength and n is an integer given by the reflection order. The stress state evolution is reflected by an interreticular distance variation of the crystallographic planes. The mean true (rational) strain $\langle\varepsilon(hkl)\rangle_{V_d}$ in the probed diffracting volume V_d, for a given measurement direction is determined from the variation between the unloaded state $d_0(hkl)$ and the loaded state, d(hkl). This deformation is connected through the Bragg law to the diffraction angles θ_0 for the reference state and θ for the stressed state by [4]:

$$\langle\varepsilon(hkl)\rangle_{V_d} = \ln\left(\frac{d(hkl)}{d_0(hkl)}\right) = \ln\left(\frac{\sin\theta_0(hkl))}{\sin\theta(hkl)}\right). \quad (2)$$

The WAXS data interpretation was limited to the {002} reflection. The lattice strains for this peak were calculated on both longitudinal (i.e., loading direction) and transverse directions. Bone tissue can be describe as a crystal dispersion material with an organic matrix, where polycrystal grains are the monocrystalline Hap platelets. In this respect, 2D WAXS diffraction patterns form concentric rings and a preferential crystallographic orientation of the crystals comes out as a strengthening of intensity in the diffraction rings over particular directions. The ensuing azimuthal intensity dependence directly relates to the predominant orientation of the mineral plates. Herman's factor [5] was used to describe and quantify crystals orientation in bone matrix by analyzing WAXS patterns. This factor, noted $F_{x/r}$, quantifies the relative orientation of a given crystallographic orientation x (in our case <001>: the Hap have a hexagonal structure and the <001> direction corresponds to the c-axis oriented along the collagen fibrils [6]) with respect to a fixed reference direction r (for example, the tensile axis). The mathematical expression of Herman's factor is given by the following relation:

$$F_{x/r} = \frac{3<\cos^2(a)> - 1}{2}. \quad (3)$$

$$\text{where } <\cos^2(a)> = \frac{\int_{\pi/2}^{\pi/2} I\cos 2\varphi \sin\varphi\, d\varphi}{\int_{\pi/2}^{\pi/2} I\sin\varphi\, d\varphi}. \quad (4)$$

a is the angle defined by the two directions x and r.

I being the intensity distribution of {hkl} diffraction peak in a given azimuthal angle φ.

The value of the Hermans factor is between -1/2 and 1.

$F_{x/r}$ = -1/2: the orientation of the crystals is perpendicular to the reference orientation,

$F_{x/r}$ = 0: an isotropic distribution of the orientation of crystals in space (uniform intensity on the ring),

$F_{x/r}$ = 1: the orientation of the crystals is parallel to the reference orientation.

SAXS data evaluation. In a SAXS experiment, the scattering of X-rays is used to obtain information about collagen fibril strain distribution and mineral crystals size. The SAXS signal intensity is based on differences in electron density on the nanostructure of bone. Therefore,

Materials Research Proceedings **6** (2018) 117-122 doi: http://dx.doi.org/10.21741/9781945291890-19

peaks obtained in SAXS indicate the periodicity of a specific phase in bone. Indeed, the variation of electron density is mainly due to those occurring between the mineral phase and the organic matrix (collagen fiber). As a two-phase material, the information on the average thickness of the mineral particles in the bone can be derived from the decay of the diffusion signal as regard to the total intensity diffused through the parameter T, thanks to Porod's law [5,7].

Here the diffusion vector $\vec{q}$ is defined as the difference between the incident and the scattered beam vector.

$$|\vec{q}| = q = \frac{4\pi}{\lambda}\sin\theta. \quad (5)$$

And according to Porod's law, the intensity of diffusion at large q values decreases with q^4.

$$\lim_{q\to\infty} I(\vec{q}) = B + \frac{P}{q^4}. \quad (6)$$

B is a background resulting from an incoherent and inelastic scattering and P is the Porod constant given by:

$$P = \lim_{q\to\infty} q^4 I(q). \quad (7)$$

Finally, T parameter is given by the following expression:

$$T = \frac{4}{\pi p}\int_0^\infty q^2 I(\vec{q})\, dq = \left(\frac{4\Phi(1-\Phi)}{s}\right). \quad (8)$$

Φ is the volume fraction of the mineralized crystals

S is the mineralized particle surface per volume unit of tissue

Assuming that the mineral phase has the shape of a uniform parallelepiped of lengths a, b and c, the expression of T is therefore:

$$T = 2(1-\Phi)\left(\frac{abc}{ab+bc+ac}\right). \quad (9)$$

The inorganic (mineral) matrix is composed of 85 % of calcium phosphate crystallized in the form of thin crystals (platelets or needles) of hydroxyapatite: $Ca_{10}(PO_4)_6(OH)_2$. These apatite crystals are generally in the form of small platelets (20 to 50 nm in length, 12 to 20 nm width and 2 to 5 nm thick). It is therefore possible to simplify the T parameter expression by assuming that $a << b, c$. the equation can be modified to:

$$T = 2a(1-\Phi). \quad (10)$$

For bone, we assume that Φ equals 0.5 [8]. Indeed, the extracellular matrix is composed by 60 to 70 % of an inorganic phase, composed essentially of hydroxyapatite crystals. Thus, T parameter gives directly the thickness of mineral particles.

Results

The map of longitudinal deformations (along loading direction) for the {002} plane family in mineral particles around the defect (marked out by dotted lines) implanted by bone graft for a load of 20 N and the related sample micro-Computed Tomograph (µ-CT), are shown in Fig. 1, for 6 weeks of regeneration. While the micro-tomography scans clearly show a complete filling of the defect after 6 weeks, the strain fields indicate that the mechanical function of the bone regarding the implant is not yet recovered at this stage of regeneration. Although the mechanical load supported by the defect is already greater at 6 weeks as compared to those at 2 and 4 weeks (not presented here) after implantation. Thus, at 6 weeks post-implantation, the regenerated bone process is not yet completed, preventing it from recovering an elastic modulus similar to that of the natural bone.

Fig. 2(a) shows the evolution of Hap plate thickness at 6 weeks post-implantation through the T parameter evaluation, as well as the distribution of their orientations thanks to Herman's orientation factor. As shown in Fig. 2(a), crystal thickness results after 6 weeks show a homogenized morphology (close thicknesses) between the crystals of the new matrix and those of the natural parts, contrary to shorter regeneration times where we notice a strong

Materials Research Proceedings **6** (2018) 117-122 doi: http://dx.doi.org/10.21741/9781945291890-19

heterogeneity between the two parts [7]. The hatched white dots in Fig 2.(a) correspond to unproductive raw data.

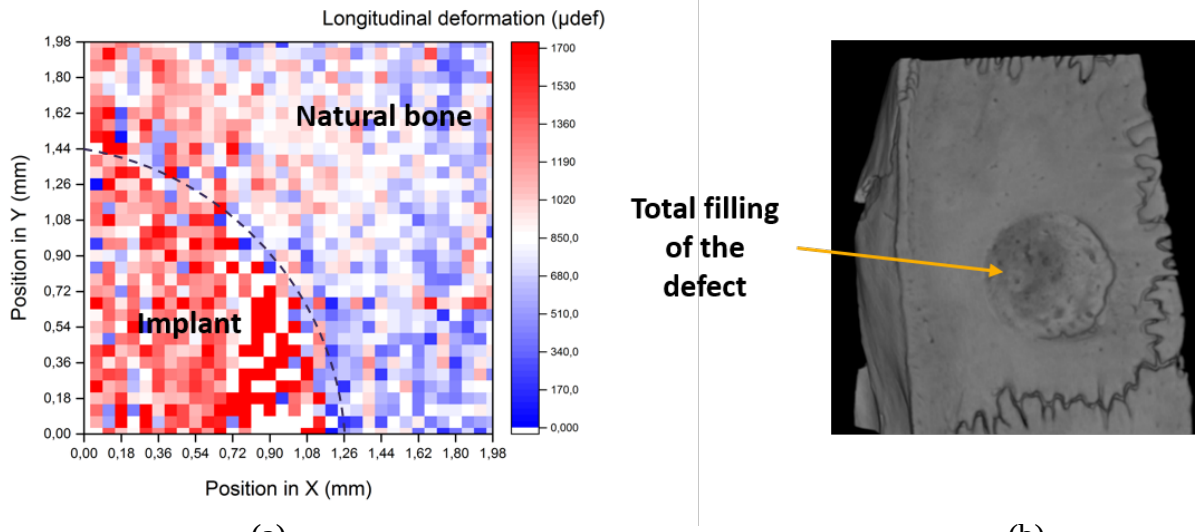

(a) (b)

Figure 1: (a) Mapping of longitudinal deformations for the {002} plane family in Hap particles around the defect implanted by bone graft for a load of 20 N, (b) associated µ-CT at 6-week post-implantation. (lattice strains are given as micro-strain (µε, units of 10^{-6})).

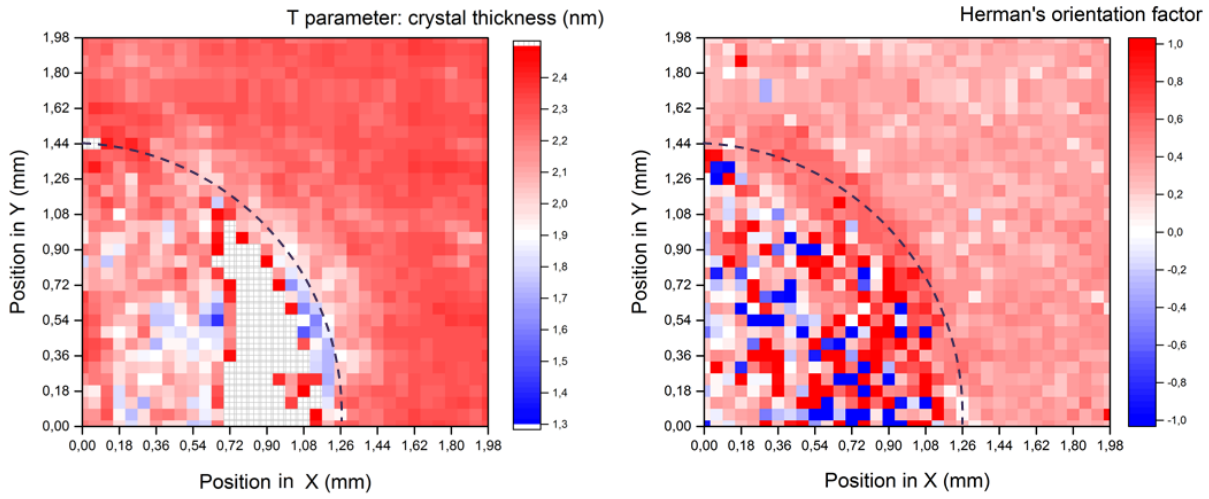

(a) (b)

Figure 2: Mapping of (a) T parameter: crystal thickness of Hap particles at 6-week post-implantation; (b) Herman's orientation factor.

Fig 2(b) presents the maps of the Herman's orientation factor at 6-week post implantation by bone graft. The synthesized tissue (organic and mineral) in the new matrix is mostly without particular orientation for this regeneration time except at the interface, where a perfect homogenization with the natural bone is highlighted. We have seen previously (Fig. 2(a)) that the crystals of the new matrix have a thickness close to that of the natural bone after 6 weeks of regeneration. On the other hand, Fig. 2(b), clearly shows that the reorganization of Hap crystals is not yet complete at this stage. This analysis is in agreement with the results from Nakano and al. [6] showing perfect homogenization between regenerated bone and natural bone at a duration of 12 weeks for a cranial bone. This suggests that, initially, bone regeneration consists in restoring the microarchitecture of the structural elements (translated here by the thickness of the

Hap crystals). In a second stage, a transformation phenomenon is initiated leading to a reorganization of the collagen fibers and mineral crystals so that they line up with those present in the natural bone.

Discussion

Bone quality is significantly altered between the natural bone and the newly formed one at this stage of regeneration (6 weeks) due to the random distribution of mineralization in the newly formed bone. Indeed, the newly formed bone has a lower mineral content, which results in a lower modulus of elasticity as shown by the high level of deformation observed in the defect compared to the natural bone at 6 weeks of regeneration (Fig. 1(a)). The analysis of the evolution of the mechanical and microstructural states during regeneration shows a correlation between the bone mechanical resistance and the microarchitecture of the crystals as well as their spatial distribution. The correlation between the size of the crystals, their organization in the newly synthesized matrix and their mechanical behavior at different stages of regeneration showed that this crystal arrangement maximizes tensile strength. It also showed that defects were initially recovered by a highly disordered tissue to be subsequently reproduced and reorganized during regeneration.

As a conclusion, osseous reconstruction takes on complex process involving a progressive set up of the bone architecture given by degree of alignment and mineral particle size, leading eventually to the microscopic and macroscopic mechanical behavior of a regenerated bone.

References

[1] Zhang, J., Wang, H., Shi, J., Wang, Y., Lai, K., Yang, X., & Yang, G. (2016). Combination of simvastatin, calcium silicate/gypsum, and gelatin and bone regeneration in rabbit calvarial defects. *Scientific reports*, *6*, 23422. https://doi.org/10.1038/srep23422

[2] Rossi, A. L., Barreto, I. C., Maciel, W. Q., Rosa, F. P., Rocha-Leão, M. H., Werckmann, J., Rossi, AM., Borojevic, R.& Farina, M. (2012). Ultrastructure of regenerated bone mineral surrounding hydroxyapatite–alginate composite and sintered hydroxyapatite. *Bone*, *50*(1), 301-310. https://doi.org/10.1016/j.bone.2011.10.022

[3] Basham, M., Filik, J., Wharmby, M. T., Chang, P. C., El Kassaby, B., Gerring, M., & Sneddon, D. (2015). Data analysis workbench (DAWN). *Journal of synchrotron radiation*, *22*(3), 853-858. https://doi.org/10.1107/S1600577515002283

[4] François, M., Ferreira, C., Reference specimens for x-ray stress analysis: The French experience. Metrologia 41 (2004) 33–40. https://doi.org/10.1088/0026-1394/41/1/005

[5] Hermans, P. H., & Weidinger, A. (1948). Quantitative x-ray investigations on the crystallinity of cellulose fibers. A background analysis. Journal of Applied Physics, 19(5), 491-506. https://doi.org/10.1063/1.1698162

[6] Nakano, T., Kaibara, K., Ishimoto, T., Tabata, Y., & Umakoshi, Y. (2012). Biological apatite (BAp) crystallographic orientation and texture as a new index for assessing the microstructure and function of bone regenerated by tissue engineering. Bone, 51(4), 741-747. https://doi.org/10.1016/j.bone.2012.07.003

[7] Fratzl, P., Schreiber, S., & Boyde, A. (1996). Characterization of bone mineral crystals in horse radius by small-angle X-ray scattering. Calcified tissue international, 58(5), 341-346. https://doi.org/10.1007/BF02509383

[8] Rinnerthaler, S., Roschger, P., Jakob, H. et et al., Scanning small angle X-ray scattering analysis of human bone sections. Calcified Tissue International, 1999. 64(5): p. 422-429. https://doi.org/10.1007/PL00005824